IEEE Access
Multidisciplinary | Rapid Review | Open Access Journal

Received November 12, 2019, accepted November 21, 2019, date of publication November 27, 2019,
date of current version December 23, 2019.

Digital Object Identifier 10.1109/ACCESS.2019.2956155

Mixing Position Estimation of AIS Mixed Signal Based on Double-Sliding Window Method

QICHAO ZHANG[1], XIN MENG[1], SHEXIANG MA[2], AND SHANSHAN LIU[2]
[1]Maritime College, Tianjin University of Technology, Tianjin 300384, China
[2]School of Electronic Engineering, Tianjin University of Technology, Tianjin 300384, China

Corresponding author: Xin Meng (mengxin@tjut.edu.cn)

This work was supported in part by the Research on Multi-User Separation and Detection Methods of Receiver Slot Conflict in Spaceborne Automatic Identification System under Grant 61371108, and in part by the Research on AIS Signal Asynchronous Interference Elimination Beamforming in Large Field of View under Grant 61601326.

ABSTRACT With the development of the shipping industry, Automatic Identification System (AIS) used for ship communication becomes more and more important. Aiming at the problem of mixing position estimation of AIS mixed signals, this paper improves the double sliding-window detection algorithm to estimate the mixing position of miscellaneous signals accurately. There is a significant difference in energy between the aliased and unmixed parts of the mixed signal. When unmixed parts just enter one of the energy detections windows, the decision function reaches its peak value by establishing a proper decision function, that is to say, the position of the beginning and end of the mixing part is estimated. The simulation results show that the proposed algorithm which is compared with the frequency and amplitude detection algorithm can achieve the mixing position estimation with low complexity and strong robustness, and the estimation accuracy is close to the Cramer-Rao Bound under the condition of the high signal-to-noise ratio.

INDEX TERMS AIS mixed signal, mixing position, decision function, double sliding-window detection.

I. INTRODUCTION

Ship Automatic Identification System (AIS) that consists of shore-based facilities and ship-borne equipment is another type of digital navigation aid system and equipment. The application of AIS equipment greatly ensures the safety of maritime traffic. In addition, the ship automatic identification system belongs to burst communication and the modulation mode is Gaussian minimum shift keying (GMSK). What is more, time division multiple access (TDMA) technology is used to divide different users into separate cells, in which each user can communicate with each other without interference. However, when the receiving device receives these signals, since the receiving range covers multiple cells, and there are multiple users in the same cell, there are factors such as position difference and signal transmission time difference between the users, which causes an increase in collision probability during signal transmission. As a result, the communication terminal may receive overlapping burst signals [1]–[3], which ultimately affects the performance of the AIS system.

For the AIS mixed-signal, the accurate estimation of the mixing position is the key to improve the effect of blind separation of the mixed signal and the signal detection. Currently, the mixing position estimation of mixed signals is realized by the signal arrival time difference. Based on Bayesian theory, [4] proposed a particle filter joint delay estimation algorithm, which can estimate the delay difference of two signals, but the algorithm is very sensitive to frequency offset changes. On this basis, [5] improved the particle filter algorithm which combined the adaptive re-sampling with the particle filter algorithm. Although the sensitivity to parameter changes is reduced, the algorithm is extremely complex. [6] proposed a parallel estimation algorithm for the delay of miscellaneous signals. This algorithm can estimate the delay parameters by using the gradient descent method to solve the analogous estimation equations of delay parameters established based on the Auto-correlation Function of mixed signals. However, this algorithm requires a sustained data length and has a harsh applicable condition. [7], [8] proposed a joint estimation algorithm based on maximum likelihood joint timing, but because it needs to know the Signal-to-Interference Ratio(SIR), its application is also very limited. A joint frequency and amplitude iterative algorithms are proposed in reference [9]. The algorithm judges whether the sampling point is mixing by comparing the sampling value between zero-crossing points with the estimated value. At the same time, the parameters of the unaligned segment are iterated to gradually improve the

The associate editor coordinating the review of this manuscript and approving it for publication was Filbert Juwono.

estimation accuracy. However, the algorithm requires a high accuracy of frequency and amplitude estimation. In addition, inspired by the working mechanism of the brain, deep neural networks [10]–[14] are designed to extract high-level feature information, which has achieved great success in many fields and specific tasks [15]–[18] such as, speech recognition [19], [20], image processing [21], natural language processing [22], and computer vision [23]. In the field of communication, signals are considered to be temporal data, which can be learned with deep learning to recognize its patterns inside [24]. Xuming Lin And Ruifang Liu[25] proposed a Deep Convolutional Network Demodulator (DCND) model and it can successfully demodulate symbol sequences from mixed signals.

As can be seen from the above, the previous processing method either needs to be implemented by means of data assistance, or the complexity is extremely high or the practicality is limited. In [26], [27], a double sliding-window detection algorithm is presented for the detection of the starting position of burst signals. The algorithm uses the energy ratio in the two energy detection windows to determine the arrival of the burst signal by determining whether the function is abrupt. The algorithm requires no prior information and is extremely insensitive to parameter changes. However, the ratio of the decision function of the algorithm and the energy detection window are not applicable when we detect the mixing position of the mixed signal.

In order to accurately estimate the starting and ending positions of mixing signals, this paper improves the traditional double-sliding window detection algorithm, splits the traditional double-sliding window into four energy detection windows, and modifies the decision function. When the unaligned part of the mixed signal just enters a certain detection window, the improved decision function just reaches the peak value, while at other times the decision function tends to be flat or the magnitude is much lower than the peak value. The improved algorithm only involves the energy ratio of signals, which not only can accurately estimate the mixing position of mixed signals under low complexity, but also maintain the excellent performance of the traditional double-sliding window detection algorithm. In conclusion, the improved algorithm in this paper can estimate with simply and accurately the starting and ending position of mixed signals. The main contribution and novelty of this paper lie in the low complexity and excellent detection performance of the improved algorithm. In addition, the improved algorithm eliminates the influence of signal delay, phase and other factors. It can accurately detect the starting and ending position of the mixing part of the mixed signal under the condition of great cost savings, which has a strong practicability.

II. GMSK MIXED SIGNAL MODEL

The AIS system operates at two frequencies, 161.975 MHZ and 162.025 MHZ, and is modulated by Gauss Filter Minimum Shift Keying (GMSK) [28]. This paper assumes that the received signal at the receiver is composed of noise and two GMSK signals with the same modulation parameters. The general expression of the mixed signal model is as follows:

$$\begin{aligned} y(t) &= A_1 s_1(t-\tau_1) + A_2 s_2(t-\tau_2) + n(t) \\ &= A_1 \cos(\omega_1 - (t-\tau_1) + \psi_1(t-\tau_1) + \theta_1) \\ &\quad + A_2 \cos(\omega_2 - (t-\tau_2) + \psi_2(t-\tau_2) + \theta_2) + n(t) \end{aligned} \tag{1}$$

In the above formula

$$\psi_1(t) = \pi \sum_{i=1}^{m} a_i^1 \int_{-\infty}^{t} h(\tau - iT) d\tau \tag{2}$$

$$\psi_2(t) = \pi \sum_{i=1}^{m} a_i^2 \int_{-\infty}^{t} h(\tau - iT) d\tau \tag{3}$$

$$h(t) = \begin{cases} \frac{1}{2T_s}\left\{Q[\frac{2\pi B}{\sqrt{\ln 2}}(t - \frac{l+1}{2}T_S)] \right. \\ \qquad \left. -Q[\frac{2\pi B}{\sqrt{\ln 2}}(t - \frac{l-1}{2}T_S)]\right\} & 0 \le t \le lT_S \\ 0 & \text{else} \end{cases} \tag{4}$$

$$Q(x) = \frac{1}{2\pi} \int_{-\infty}^{t} e^{-\frac{t^2}{2}} dt \tag{5}$$

In the above formula, ω is the radian frequency, $\psi(t)$ is the phase function, τ_1 and τ_2 are the delay of two signals respectively. θ_1 and θ_2 are their respective initial phases. $n(t)$ represents zero mean Gaussian white noise. $\{a_i = \pm 1\}$ in Eq. (2) and Eq. (3) represent the respective transmission bit information. T_s represents the symbol period.$h(t)$ is defined as the impulse response function of the Gaussian filter. In Eq. (4), $B = 3dB$ equivalent bandwidth of the Gaussian filter. L denotes the number of cycles in which the base-band response lasts.

A. BURST DETECTION OF BURST SIGNALS BY TRADITIONAL DOUBLE SLIDING WINDOW METHOD

In this paper, the mixing position detection of mixed signals is based on the double-sliding window detection algorithm, which has outstanding performance in detecting burst signals. Compared with continuous signals, burst signals have higher anti-interception and anti-interference ability, but the signal is sent randomly [29]. So, it is necessary to detect the burst signal. In this paper, the detection of AIS signals also belongs to the burst signal. For this reason, the principle of the traditional algorithm is firstly introduced to facilitate the understanding of the improved algorithm. The principle block diagram of the traditional double-sliding window detection method is shown in Fig. 1:

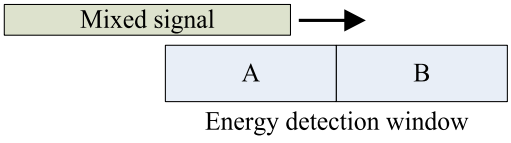

FIGURE 1. Principle Diagram of Double Sliding Window Detection Method.

The detection of the burst position depends on the change of signal energy in Windows A and B. The lengths of windows A and B are L. At time n, the energy in the two windows is respectively:

$$a_n = \sum_{i=1}^{L} a_{ni} a_{ni}^* = \sum_{i=1}^{L} |a_{ni}|^2 \tag{6}$$

$$b_n = \sum_{i=1}^{L} b_{ni} b_{ni}^* = \sum_{i=1}^{L} |b_{ni}|^2 \tag{7}$$

The decision function is:

$$m_n = \frac{a_n}{b_n} + \frac{b_n}{a_n} \tag{8}$$

In Eq. (6) and Eq. (7), a_n and b_n respectively represent the energy detected in the energy detection the window A and B at time n. The traditional decision function is $m_n = a_n/b_n + b_n/a_n$. When two energy detection windows only contain noise, the response of m_n is flat. As the edge of the available data reaches the window A, the energy in A keeps increasing and the ratio of a_n/b_n increases. However, the value of b_n/a_n is much smaller than a_n/b_n, which can be ignored until the window A is full of valid data. At this time,m_n reaches a certain maximum value, which corresponds to the starting position of the burst signal. When valid data starts to leave window A, the energy in window A is always reduced, and the ratio of b_n/a_n is increasing. At this time, the ratio of a_n/b_n is much smaller than that of b_n/a_n, which can be neglected. Until valid data just leave the window A. m_n reaches another maximum value, which corresponds to the end position of the burst signal. Thus, the burst position detection of the burst signals can be completed.

However, the traditional double-sliding window method is not suitable for detecting the mixing position of mixed signals. At time n, the overlapping part of the mixed signal just enters the window A completely. At this time, the value of a_n/b_n is not the maximum, and the value of b_n/a_n can't be ignored. Because the unmixed part of the mixing signal has entered the window B, the energy in the window B can't be overlooked, which shows that the traditional double-sliding window detection method is not suitable for the detection of the overlapping position of the mixed signal.

III. OVERLAPPING POSITION ESTIMATION OF MIXED SIGNALS

For AIS signals, the determination of mixing position is an effective method to reduce the complexity of the blind separation process and the bit error rate of the decoding process. Based on the double-sliding window method to different windows based on signal energy ratio, according to the decision function to estimate the value of sudden emergency of position signal, but the conventional algorithm has insufficient detection [30]. When not mixing part into the energy detection window, corresponding decision function can't enlarge not mixing energy, lead to the final decision function can't response on the part of the signal. Take into account this, this paper improves the traditional double-sliding window detection method. Based on this, this paper improves the customary double-sliding window detection method. By expanding the energy detection window and optimizing the decision function, the mixing position of mixed signals can be estimated with high accuracy.

A. ESTIMATION OF MIXED SIGNALS BY IMPROVED ALGORITHMS

Traditional double-sliding window detection can only detect the initial position of the burst signal. However, the traditional method is not applied when the mixed signal has a relative delay and it needs to estimate the position of the mixed signal. In order to detect the mixing position of the mixed signal, the energy detection window is expanded to four and the decision function is redefined. The schematic diagram of the improved sliding window is illustrated in Fig. 2 below.

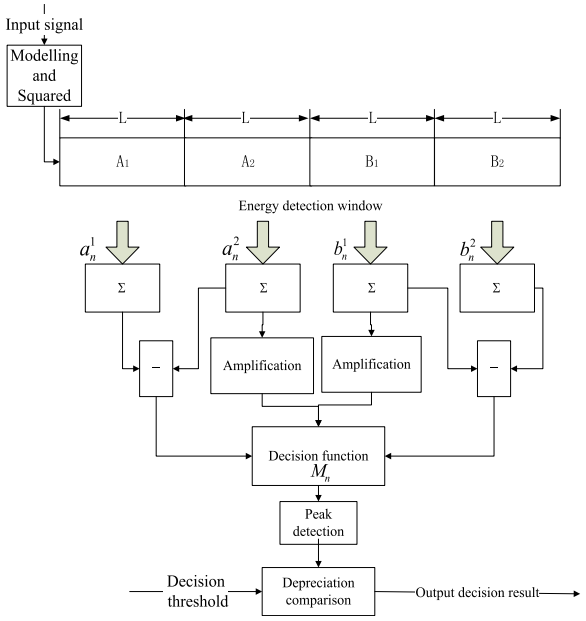

FIGURE 2. Improvement of Double Window Detection Principle Diagram.

As showed in Fig. 2, the traditional energy detection window with a length of 2L is extended to the new window with a length of 4L. The new detection window is divided into four segments of equal length, and each segment is defined as A_1, A_2, B_1, and B_2, respectively. And the energy to the energy detection window is redefined as a_n^1, a_n^2, b_n^1 and b_n^2.

There are:

$$a_n^1 = \sum_{i=1}^{L} a_{ni}^1 (a_{ni}^1)^* = \sum_{i=1}^{L} \left|a_{ni}^1\right|^2 \tag{9}$$

$$a_n^2 = \sum_{i=L+1}^{2L} a_{ni}^2 (a_{ni}^2)^* = \sum_{i=L+1}^{2L} \left|a_{ni}^2\right|^2 \tag{10}$$

$$a_n' = a_n^1 + a_n^2 \tag{11}$$

$$b_n^1 = \sum_{i=2L+1}^{3L} b_{ni}^1 (b_{ni}^1)^* = \sum_{i=2L+1}^{3L} \left| b_{ni}^1 \right|^2 \tag{12}$$

$$b_n^2 = \sum_{i=3L+1}^{4L} b_{ni}^2 (b_{ni}^2)^* = \sum_{i=3L+1}^{4L} \left| b_{ni}^2 \right|^2 \tag{13}$$

$$b_n' = b_n^1 + b_n^2 \tag{14}$$

The new decision function is redefined as:

$$M = \left| \frac{(a_n^2)^{10}(a_n^1 - a_n^2)}{a_n^1} \right| + \left| \frac{(b_n^1)^{10}(b_n^2 - b_n^1)}{b_n^2} \right| \tag{15}$$

Parameters a_n^1, a_n^2, b_n^1 and b_n^2 in Eq. (9), Eq. (10), Eq. (12) and Eq. (13) respectively represent the total energy detected in the four detection Windows at time n. a_{ni}^1, a_{ni}^2, b_{ni}^1 and b_{ni}^2 respectively represent symbols in the four-segment detection window from the i-th symbol to the end of the detection window at the time n, and i denotes the respective starting positions of each detection window. $*$ indicates conjugate.

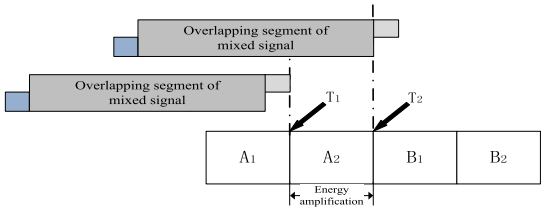

(a) Procedure Diagram of Staring Point Location Detection of Overlapping Segment.

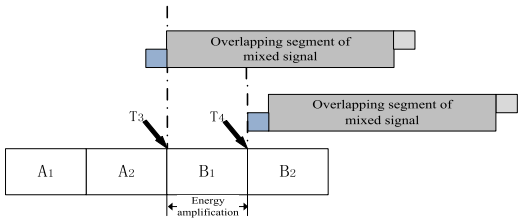

(b) Procedure Diagram of End Point Location Detection of Overlapping Segment.

FIGURE 3. (a) Procedure Diagram of Staring Point Location Detection of Overlapping Segment. (b) Procedure Diagram of End Point Location Detection of Overlapping Segment.

When the four windows only contain the noise, it is obvious that the response of M is flat. As shown in Fig. 3(a)(b), when the signal is in the position before T_1 and after T_4. Although the energy difference in the adjacent window is large, there is only noise in the energy amplification window at this time, and the magnitude of amplification does not affect the decision result. When the signal is between T_2 and T_3, the signal in the adjacent window is basically the same, the existence of $(a_n^1 - a_n^2)$ and $(b_n^2 - b_n^1)$ in the decision function make the decision result change very small. When the signal is between T_1 and T_2 or T_3 and T_4, the energy in the adjacent window is inconsistent, and the amplified non-overlapping part of the signal energy will directly affects the decision result. It is worth mentioning that the difference in the magnitude of the energy levels in the adjacent window at this time is small, so it will not affect the magnitude of the decision result. Taking the time between T_1 and T_2 as an example, there is only noise in the window B at this time, so the right half $(b_n^1)^{10}(b_n^2 - b_n^1)/b_n^2$ of the decision function can be ignored. The energy of the unmixed part entering the window A_2 is amplified, and the energy in A_1 is also increased. However, the ratio of A_1 increase is less than the magnitude of the amplification in A_2, so the decision value is gradually increased. When the unmixed portion just enters A_2 completely and the decision function reaches the peak value, meanwhile the initial position of the overlapping part of the mixed signal can be judged. It is also possible to determine the end position of the mixing portion. When the value of the decision function M reaches a peak, the beginning of the overlapping portion of the signal can be determined. This allows the mixing position of the mixed signal to be detected.

IV. SIMULATION RESULTS AND ANALYSIS

Determination of the signal energy amplification index in the decision function. The algorithm uses the ratio of signal energy to determine the mixing position of the mixed signal. We consider that the algorithm is more affected by the signal-to-noise ratio. Through simulation experiments, it is found that when the SNR is reduced to $9dB$, the signal energy amplification index is at least above 7. Only at the beginning and end of the mixing position can be the decision function show obvious mutation effect.

The simulation uses two co-frequency GMSK mixed signals with a rate of 9600B. The amplitude is 1, and the time-bandwidth is $BT = 0.4$. The frequency offset and phase are 0. The information sequence has a length of 256 bits and an oversampling rate of 10, for a total of 2560 points. The length of the individual energy detection windows before and after the improvement is 64. The estimation effect of the decision function was observed under different SNR and different magnified index. In order to ensure the practicability of the algorithm as far as possible, we reduced the signal to noise ratio to $9dB$ and set the magnified index at 9 and 10.

As can be seen from Fig. 4, when the magnified index is set to 9, although the decision function will have abrupt changes at the corresponding position. There will be non-quantitative abrupt changes in the intermediate process, which will have a certain impact on the final judgment.

When the SNR increases to $15dB$, the magnified index is set to 6 and 8, and the simulation effect is shown in the Fig. 5. From the simulation results, it can be concluded that when the magnified index is 6, there is an obvious mutation at the starting and ending position of mixed signals. But there are also mutations at the point where the signal comes and goes. This phenomenon is caused by the fact that the energy of the unmixed part of the signal is amplified too low. When the magnified index is 8, the expected judgment effect can be achieved.

When the SNR increases to $20dB$, the magnified index is 4 and 6. The simulation result is shown in Fig. 6.

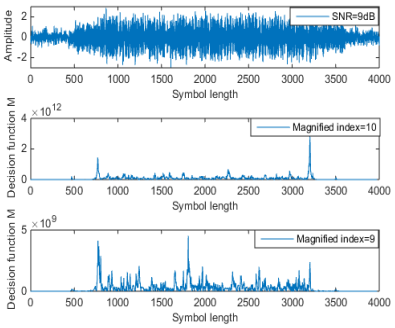

FIGURE 4. Estimation of magnification index.

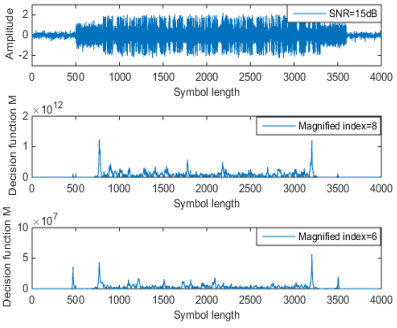

FIGURE 5. Estimation of magnification index.

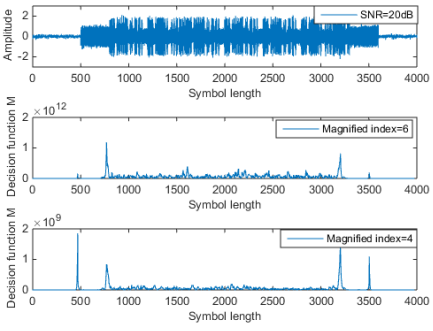

FIGURE 6. Estimation of magnification index.

Similarly, when the amplification index is insufficient, the decision function changes as the signal arrives and leaves. When the magnified index reaches 6, the estimation effect can be better achieved.

In summary, when the SNR is relatively low. If the expected estimation effect is to be achieved, it is necessary to amplify the power of the un-overlapped part of the mixed signal by a larger exponent. With the increase of signal-to-noise ratio, the energy of the signal is much than the energy of the noise. The magnitude of amplification is reduced. In general, we set the magnifying exponent of the decision function to 10.

Simulation verifies the practicability and superiority of the algorithm. The other parameters are consistent with simulation 4. The signal-to-noise ratio (SNR) is set to $20dB$, and the magnified index is set to 10. The mixing position of the mixed signal is compared with that estimated by the decision function.

As can be seen from Fig. 7, at the beginning and end of the mixing of the mixed signal, the decision function will reach its respective peak and reach the order of 10^{12} orders of magnitude. Between the mixing start and end positions, the mixed signal energy in the window A_1 and A_2 is much larger than the noise. At this time, the result of $(a_n^1 - a_n^2)$ is close to zero but not be negligible, and the $(a_n^2)^{10}/a_n^1$ ratio is equivalent to $(a_n^1)^9$, so the intermediate fluctuation can be observed.

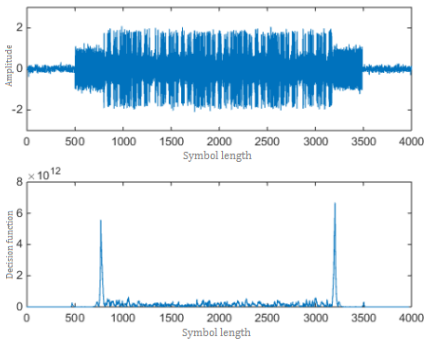

FIGURE 7. Mixing position detection of mixed signals.

The other simulation parameter settings are consistent with the above, and the improved double-sliding window algorithm is compared with the frequency amplitude algorithm in [9] under different relative delay conditions. 500 Monte Carlo experiments are performed for each point. The error is used as the verification parameter, and the results are shown in Fig. 8 and Fig. 9. In order to simplify the representation in the following simulation, the Frequency And Amplitude Detection algorithm is abbreviated as Frequency-Amplitude, and the Double-sliding Window Detection algorithm is abbreviated as sliding-window.

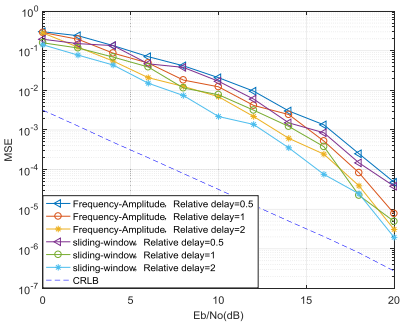

FIGURE 8. Performance comparison of overlapping position detection with relatively small delay.

It can be reached from the simulation results that when the relative delay difference of the mixed signal is small, the detection effect of the improved algorithm is not ideal.

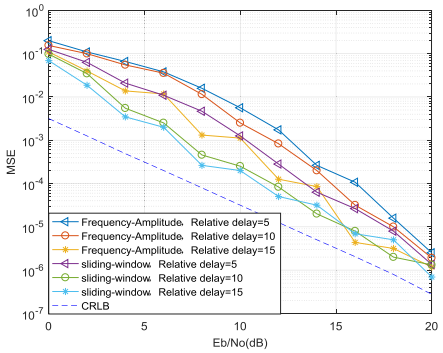

FIGURE 9. Performance comparison of overlapping position detection with large relative delay.

But it is obviously better than the frequency amplitude detection. When the relative delay difference of the mixed signal is large, the performance of the improved double-sliding window algorithm is significantly better than the frequency amplitude detection algorithm and close to the Cramer-Rao bound because the frequency amplitude detection algorithm requires a priori data to estimate the frequency and amplitude and then iterate, and the estimation accuracy of the frequency and amplitude is very high.

The other parameter settings are consistent with the experimental one, and the relative delay difference is set to 15 symbols, and the performance of the improved algorithm is verified under different frequency offset and phases. It can be consulted on the simulation results below that the improved double-sliding window detection method is insensitive to parameter changes and has good robustness.

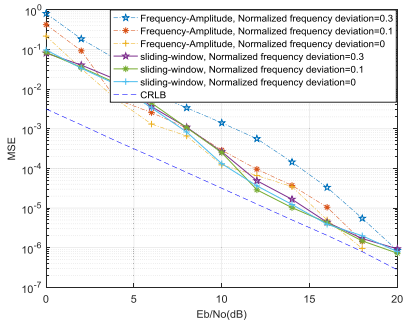

FIGURE 10. Overlap position detection at different frequency offsets.

It can be seen from Fig. 10 and Fig. 11 that the frequency offset and phase have no significant effect on the results of the proposed algorithm, but have a greater impact on the frequency amplitude detection algorithm because the algorithm principle of this paper is based on the ratio of signal energy. Changing the parameter frequency and phase does not have a significant effect on the energy of the signal. The frequency amplitude algorithm needs to estimate the frequency and amplitude of the original signal more accurately, and then iteratively realize the estimation of the mixing position.

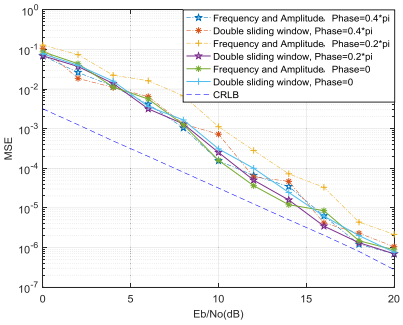

FIGURE 11. Overlap position detection under different initial phases.

The changes of the initial phase and frequency offset of the signal will have a greater impact on the original signal model. The ratio of the aliased position estimation algorithm based on energy is more robust than the frequency amplitude detection algorithm.

It can be intuitively seen from the above simulation results that the two maximum values of the decision function of the improved algorithm correspond exactly to the mixing start and end positions of the mixed signal, and the magnitude of the maximum value reaches $7.11 * 10^{12}$. This can greatly reduce the impact of noise on the final result. From this, the effectiveness of the improved double-sliding window detection method for estimating the position of the mixed signal mixing segment can be obtained. On the basis of the estimation of the mixed signal mixing start and end position, the same initial simulation conditions are set, and the performance of the improved double-sliding window detection method and Frequency-Amplitude detection algorithm is compared. It can be seen from the simulation results that the improved algorithm has higher estimation accuracy, lower complexity, stronger robustness, and more importantly, blind estimation without prior information. Moreover, with the signal-to-noise ratio increasing, its performance is getting better and better. This is because the magnitude of the signal energy is much larger than the noise energy, and the resulting error of the decision function is smaller. It can be seen from Fig. 6 that when the relative delay difference of the mixed signal reaches 15 symbols, the mean square error of the mixed position estimation reaches $10^{-6.2}$ orders of magnitude very close to the Cramer-Rao bound.

V. CONCLUSION

In this paper, the problem of mixing position estimation of mixed signals is improved. The double-sliding window detection method is improved. The traditional two energy detection windows are refined into four, and the decision function is redefined. When the unaligned part of the signal completely enters the amplified energy detection window, the decision function just reaches the peak value; and at other times, the magnitude of the decision result is reduced by

multiplying the energy difference in the adjacent window. The closer the energy of the adjacent window is to the effect on the magnitude of the final decision function, the more significant the effect is when the decision function reaches its peak value. The improved algorithm can not only estimate the mixing position of the AIS mixed signal, but also the accuracy and complexity of the estimation are better than the frequency amplitude detection algorithm. The simulation results show that the proposed algorithm can accurately estimate the mixing position of the AIS mixed signal, and the estimation accuracy is close to the Cramer-Rao bound when the signal-to-noise ratio is high, which is not sensitive to the change of parameters and has strong robustness. The algorithm designed in this paper can be used in the pretreatment stage of the blind separation of mixed signals. If the overlapping part of the mixed signal is less and only blind separation is carried out for the overlapping part, the separation effect can be greatly improved. However, this method is also limited by the power of the signal. If the power difference between the mixed signals is large, the detection effect will be poor, so this method still has a high research value. And i, in the future, will consider adding a deep learning algorithm to further improve the accuracy of the estimation.

REFERENCES

[1] L. Shan, S. Ma, X. Meng, and L. Zhou, "Interference suppression of partially overlapped signals using GSVD and orthogonal projection," *IEICE Trans. Commun.*, vol. E102.B, no. 5, pp. 1055–1060, 2018.

[2] N. D. Merchant, M. J. Witt, P. Blondel, B. J. Godley, and G. H. Smith, "Assessing sound exposure from shipping in coastal waters using a single hydrophone and automatic identification system (AIS) data," *Mar. Pollut. Bull.*, vol. 64, no. 7, pp. 1320–1329, Jul. 2012.

[3] P. Burzigotti, A. Ginesi, and G. Colavolpe, "Advanced receiver design for satellite-based automatic identification system signal detection," *Int. J. Satell. Commun. Netw.*, vol. 30, no. 2, pp. 52–63, Mar./Apr. 2012.

[4] K. H. Knuth and H. G. Vaughan, Jr., "Convergent Bayesian formulations of blind source separation and electromagnetic source estimation," in *Maximum Entropy and Bayesian Methods Garching, Germany* (Fundamental Theories of Physics), vol. 105. 2015, pp. 217–226.

[5] W.-J. Tan, J.-Z. Yang, L. Wang, and D.-Z. Zhao, "Hand gesture tracking method based on Kalman filter and skin color feature," *J. Northeastern Univ.*, vol. 34, no. 4, pp. 474–477, 2013.

[6] L.-G. Shi, Z.-G. Wang, and W.-M. Xiong, "SNR estimation algorithm for GMSK+PN signal," *Syst. Eng. Electron.*, vol. 38, pp. 26–30, Jan. 2016.

[7] H. Zhang, Y. Yang, G. Xin, and S. Du, "PSP blind separation algorithm for GMSK mixed signals," *J. Terahertz Sci. Electron. Inf. Technol.*, vol. 13, no. 1, pp. 142–147, Jan. 2015.

[8] Y.-F. Zhao, Y.-J. Cao, and X.-C. Dai, "Time delay estimation for single-channel mixed digital communication signals," *J. Signal Process.*, vol. 31, no. 2, pp. 161–169, 2015.

[9] C. Hu, Y. Yang, Y. Zhu, and G. Xin, "Hybrid position iterative estimation algorithm for burst GMSK mixing signals," *J. Data Acquisition Process.*, vol. 29, pp. 421–426, May 2014.

[10] A. Toshev and C. Szegedy, "DeepPose: Human pose estimation via deep neural networks," in *Proc. IEEE Conf. Comput. Vis. Pattern Recognit.*, Jun. 2013, pp. 1653–1660.

[11] K. A. Darabkh, L. Haddad, S. Z. Sweidan, M. Hawa, R. Saifan, and S. H. Alnabelsi, "An efficient speech recognition system for arm is abled students based on isolated words," *Comput. Appl. Eng. Educ.*, vol. 26, no. 2, pp. 285–301, 2017.

[12] R. Balestriero and R. Baraniuk, "Deep neural networks," Oct. 2017, *arXiv:1710.09302*. [Online]. Available: https://arxiv.org/abs/1710.09302

[13] Y. Sun, H. Chockler, X. Huang, and D. Kroening, "Explaining deep neural networks using spectrum-based fault localization," pp. 1–12, Jan. 2019.

[14] G. Montavon, W. Samek, and K.-R. Müller, "Methods for interpreting and understanding deep neural networks," *Digit. Signal Process.*, vol. 73, pp. 1–15, Feb. 2018.

[15] G. Alpaydin, "An adaptive deep neural network for detection, recognition of objects with long range auto surveillance," in *Proc. IEEE 12th Int. Conf. Semantic Comput. (ICSC)*, Laguna Hills, CA, USA, Jan./Feb. 2018, pp. 316–317.

[16] X. Chang, T. Xiang, and T. M. Hospedales, "Scalable and effective deep CCA via soft decorrelation," in *Proc. IEEE Conf. Comput. Vis. Pattern Recognit. (CVPR)*, Jun. 2018, pp. 1488–1497.

[17] A. G. Howard, "Some improvements on deep convolutional neural network based image classification," in *Proc. ICLR*, Dec. 2013, pp. 1–6.

[18] S. Chollampatt and H. T. Ng, "A multilayer convolutional encoder-decoder neural network for grammatical error correction," in *Proc. 32nd AAAI Conf. Artif. Intell.*, Apr. 2018, pp. 5755–5762.

[19] J. P. Dominguez-Morales, Q. Liu, R. James, D. Gutierrez-Galan, A. Jimenez-Fernandez, S. Davidson, and S. Furber, "Deep spiking neural network model for time-variant signals classification: A real-time speech recognition approach," in *Proc. Int. Joint Conf. Neural Netw. (IJCNN)*, Jul. 2018, pp. 1–8.

[20] M. Cai and J. Liu, "Maxout neurons for deep convolutional and LSTM neural networks in speech recognition," *Speech Commun.*, vol. 77, pp. 53–64, Mar. 2016.

[21] M. Bublin, "Machine learning for distributed acoustic sensors, classic versus image and deep neural networks approach," Apr. 2019, *arXiv:1904.11546*. [Online]. Available: https://arxiv.org/abs/1904.11546

[22] Y. Qian, M. Bi, T. Tan, and K. Yu, "Very deep convolutional neural networks for noise robust speech recognition," *IEEE/ACM Trans. Audio, Speech, Language Process.*, vol. 24, no. 12, pp. 2263–2276, Dec. 2016.

[23] S. Mukhopadhyay, "Deep learning and neural networks," Tech. Rep., 2018.

[24] D. Miyashita, S. Kousai, T. Suzuki, and J. Deguchi, "A neuromorphic chip optimized for deep learning and CMOS technology with time-domain analog and digital mixed-signal processing," *IEEE J. Solid-State Circuits*, vol. 52, no. 10, pp. 2679–2689, Oct. 2017.

[25] M. Crepaldi, M. R. Casu, M. Graziano, and M. Zamboni, "A mixed-signal demodulator for a low-complexity IR-UWB receiver: Methodology, simulation and design," *Integr. VLSI J.*, vol. 42, no. 1, pp. 47–60, 2009.

[26] F. Lieb, H.-G. Stark, and C. Thielemann, "A stationary wavelet transform and a time-frequency based spike detection algorithm for extracellular recorded data," *J. Neural Eng.*, vol. 14, no. 3, 2017, Art. no. 036013.

[27] J.-R. Xin, J. Wan, S.-H. Chen, and J. Cheng, "Research on receiving technology based on blind signal separation for satellite MIMO communication system," *J. Syst. Simul.*, vol. 3, pp. 484–488, Mar. 2013.

[28] X. J. Liu, S. X. Ma, and X. Meng, "Frequency-offset estimation of satellite-based AIS signals," *Adv. Mater. Res.*, vols. 765–767, pp. 2732–2735, Sep. 2013.

[29] D. A. Guimarães and C. H. Lim, "Sliding-window-based detection for spectrum sensing in radar bands," *IEEE Commun. Lett.*, vol. 22, no. 7, pp. 1418–1421, Jul. 2018.

[30] M. Al-Jarrah, K.-H. Park, A. Al-Dweik, and M.-S. Alouini, "Error rate analysis of amplitude-coherent detection over Rician fading channels with receiver diversity," Feb. 2019, *arXiv:1902.01812*. [Online]. Available: https://arxiv.org/abs/1902.01812

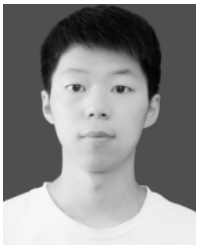

QICHAO ZHANG received the B.S. degree from the Tianjin University of Technology and Education, in 2017, where he is currently pursuing the M.S. degree with the School of Maritime. His research interest includes on-board AIS signal processing.

XIN MENG received the master's degree from the Tianjin University of Technology, where he is currently pursuing the Ph.D. degree in communication engineering. His research interests include maritime communication and navigation technology.

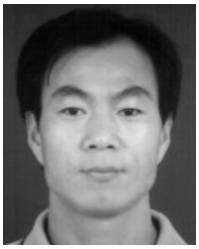

SHEXIANG MA received the Ph.D. degree in technical science degree from the School of Information and Communication Engineering, College of Xi'an Jiao Tong University, in 2003. He is currently a Professor with the School of Electrical and Electronic Engineering, Tianjin University of Technology, Tianjin, China. His research interests include array signal processing and mobile communication.

SHANSHAN LIU is currently pursuing the master's degree with the School of Electrical and Electronic Engineering, Tianjin University of Technology. Her research interest includes ship trajectory tracking and prediction.